Thermochronology of the Salt Spring fault: Constraints on the evolution of the South Virgin–White Hills detachment system, Nevada and Arizona, USA

Charles Verdel*, Nathan Niemi, and Ben A. van der Pluijm
Department of Geological Sciences, University of Michigan, Ann Arbor, Michigan 48109, USA

ABSTRACT

We present new clay mineralogy and muscovite and illite $^{40}Ar/^{39}Ar$ data from fault gouge and immediately adjacent wall rocks from the Salt Spring fault, the central portion of the Miocene South Virgin–White Hills detachment system in southern Nevada and northern Arizona. In combination with a wealth of published regional thermochronology data, we find that useful age information can be obtained from $^{40}Ar/^{39}Ar$ step-heating spectra of fine-grained clays in both sedimentary rocks and fault gouge derived from them. This information can be used to investigate the provenance of detrital clays in low-grade sediments, the source of clays in fault gouge, and potentially to constrain thermal histories.

A new muscovite $^{40}Ar/^{39}Ar$ age from the footwall near the Salt Spring fault is ca. 900 Ma, in contrast with previously reported ages of ca. 90 Ma from near the South Virgin–White Hills detachment system at Gold Butte, Nevada, located 20 km along strike to the north. This discrepancy in muscovite cooling ages supports prior interpretations of significant along-strike variations in the magnitude of footwall exhumation. $^{40}Ar/^{39}Ar$ data from clay-size sediment in a supradetachment basin at the Salt Spring Wash area show no influence from detrital ca. 900 Ma or older muscovite, but do show an influence from detrital muscovite with Cretaceous apparent ages, suggesting that these sediments were derived from Gold Butte to the north, and not from directly updip areas to the east. These observations suggest a Miocene paleotopographic configuration wherein Gold Butte formed an upland area that shed detritus southward into the supradetachment basin during exhumation of the Salt Spring footwall.

Fault gouge from the Salt Spring detachment is similar to fine-grained sediment from the adjacent supradetachment basin both in terms of clay mineralogy and $^{40}Ar/^{39}Ar$ results. The gouge is rich in illite and smectite, clays that have low frictional coefficients, are relatively impermeable, and would have reduced the shear strength of the detachment at shallow depths. Apatite grains entrained in the gouge have a mean fission-track age of 15 Ma and mean track lengths that are statistically indistinguishable from previously published data from footwall samples. Collectively, these observations suggest that clay-rich gouge along this segment of the fault formed principally by scraping and incorporating clays and other minerals from the base of the supradetachment basin and that the fault zone did not experience temperatures measurably greater than the footwall.

INTRODUCTION

The Basin and Range Province of the western U.S. is one of the world's best examples of intracontinental rifting (e.g., Hamilton and Myers, 1966; Anderson, 1971; Wernicke et al., 1988; McQuarrie and Wernicke, 2005; Anderson and Beard, 2010). The region includes normal faults that dip at low to moderate angles (detachments), which, in some cases, have exhumed mid-crustal rocks in their footwalls (e.g., Armstrong, 1972, 1982; Crittenden et al., 1980; Lister and Davis, 1989; Hoisch and Simpson, 1993; Wright and Troxel, 1993). Low- and medium-temperature thermochronometers have been used extensively to determine the timing and rate of exhumation in these areas of Tertiary extension (e.g., Fitzgerald et al., 1991; Foster et al., 1993; Holm and Dokka., 1993; Miller et al., 1999; Brady, 2002; Stockli et al., 2002), and the deep, ductile portions of detachments have also been described and studied in considerable detail (e.g., Davis, 1983; Glazner and Bartley, 1991; Hurlow et al., 1991; Fricke et al., 1992).

Detachment faulting in the shallow, brittle regime is a component of Basin and Range extension that has received less attention, despite its potential importance for understanding the mechanical properties and evolution of detachment fault systems. In particular, shallow portions of detachments often include mechanically weak, clay-rich fault gouge (Cowan et al., 2003; Hayman, 2006; Haines et al., 2009), which may permit slip at angles less than predicted by Andersonian fault theory (Anderson, 1942; Numelin et al., 2007; Ikari et al., 2009; Boulton et al., 2009). In some cases the generation of gouge in Basin and Range detachments appears to be associated with the circulation of hydrous fluids (Spencer and Welty, 1986; Pavlis et al., 1993; Hayman, 2006; Michalski et al., 2007). Elevated pore pressure and hydrothermal mineralization promoting cohesion are, in their own rights, mechanisms by which slip could occur on frictionally weak detachments oriented unfavorably with respect to the regional stress direction (e.g., Axen, 1992; Axen and Selverstone, 1994; Healy, 2009). Observations from shallow faults that bear on the sources of clays in fault gouge, the compositions of these clays and their mechanical properties, and the physical conditions (i.e., temperature and pressure) under which gouge forms are therefore important for a more complete understanding of the mechanical behavior of detachment faulting.

Here we address these issues utilizing field observations, clay mineralogy data, and low-temperature thermochronology in the vicinity of the Salt Spring fault of northern Arizona (Figs. 1 and 2). We focus on this fault because (1) it is part of the regionally important South Virgin–White Hills detachment system

*Present address: Department of Geology, University of Kansas, Lawrence, Kansas 66045, USA; Email: cverdel@ku.edu.

Geosphere; June 2011; v. 7; no. 3; p. 774–784; doi:10.1130/GES00616.1; 7 figures; 1 supplemental table.

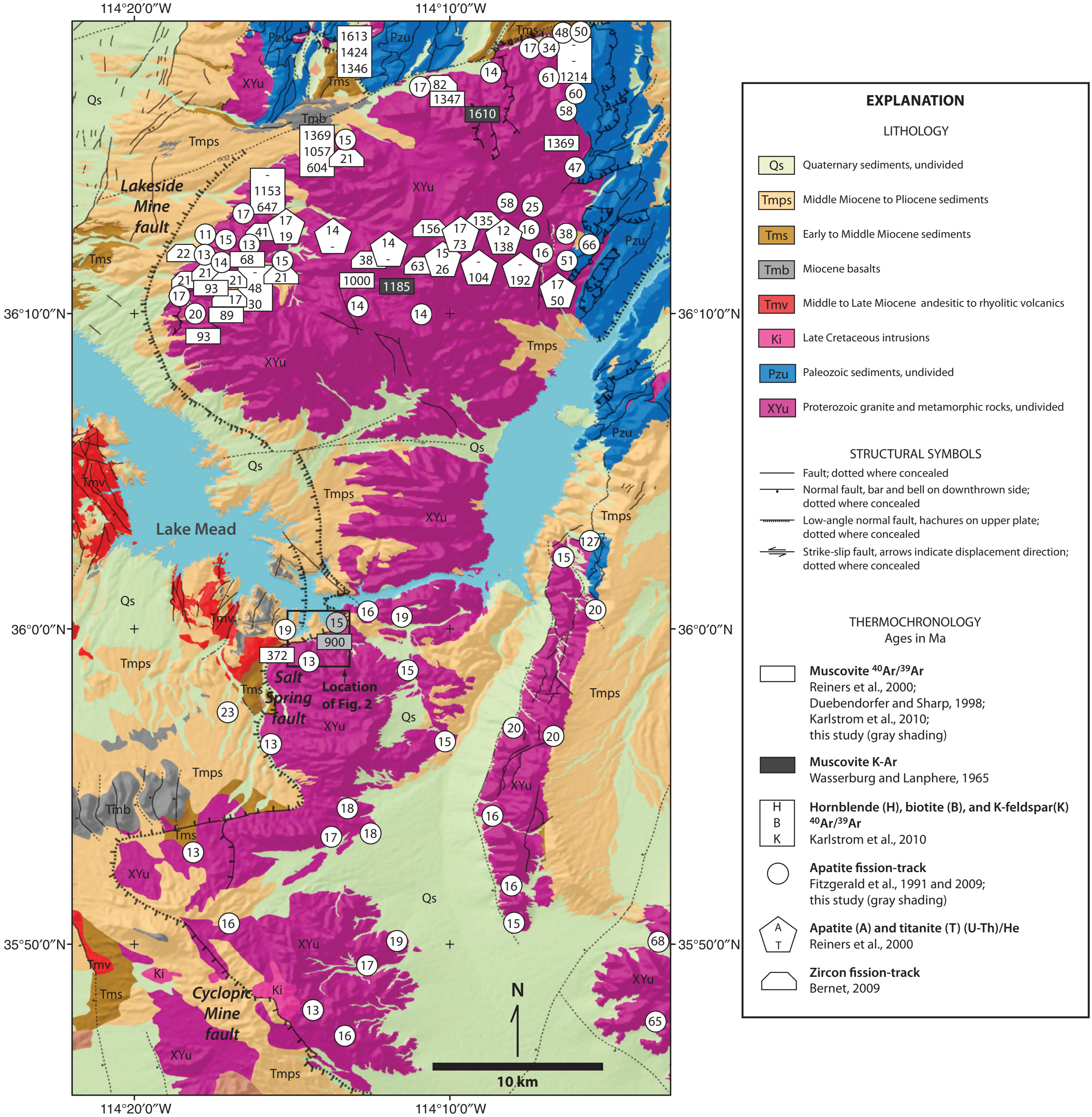

Figure 1. Geologic map of the South Virgin Mountains–White Hills area (after Felger and Beard, 2010) illustrating previous and new thermochronology results (Wasserburg and Lanphere, 1965; Fitzgerald et al., 1991, 2009; Reiners et al., 2000; Bernet, 2009; Karlstrom et al., 2010). Locations of some thermochronology samples in the Gold Butte block have been shifted slightly for clarity.

(SVWHD); (2) exhumation of the footwall of the SVWHD is well constrained by low-temperature thermochronology (Fitzgerald et al., 1991, 2009; Reiners et al., 2000, 2002; Bernet, 2009; Karlstrom et al., 2010); and (3) local exposures permit direct observation of the fault zone (Duebendorfer and Sharp, 1998; Howard, 2003; Howard et al., 2010). Our data come from the Salt Spring fault and the rocks immediately above and below it, and have implications for the regional pattern of exhumation along this detachment system.

SOUTH VIRGIN–WHITE HILLS DETACHMENT SYSTEM

The 80-km-long SVWHD of southern Nevada and northern Arizona is an along-strike alignment of three west-dipping normal fault

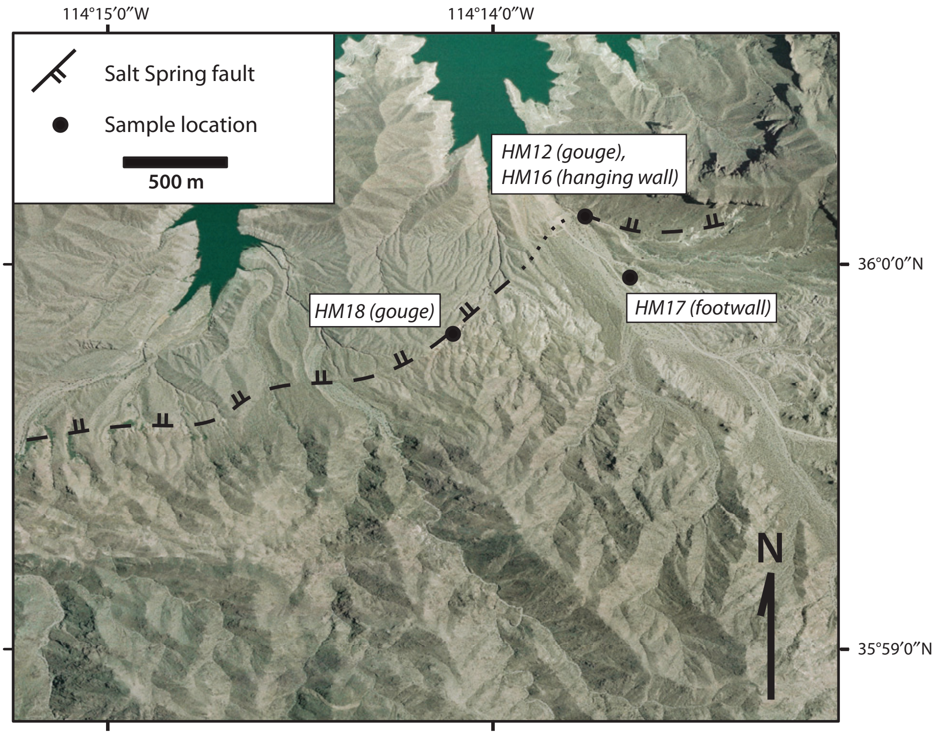

Figure 2. Air photo showing studied portion of the Salt Spring fault and footwall, hanging wall, and fault gouge sample locations.

segments: the northern Lakeside Mine segment, the central Salt Spring fault, and the southern Cyclopic Mine segment (Fig. 1; Duebendorfer and Sharp, 1998; Brady et al., 2000; Fitzgerald et al., 2009; Duebendorfer et al., 2010). Extension accommodated by the northern segment (the Lakeside Mine fault) exhumed an east-tilted block of Proterozoic crystalline rocks at Gold Butte, Nevada (Wernicke and Axen, 1988; Fryxell et al., 1992). Multiple low-temperature thermochronology investigations have documented a period of rapid Middle Miocene cooling of the Gold Butte tilted block (Fitzgerald et al., 1991, 2009; Reiners et al., 2000, 2002; Bernet, 2009). The Lakeside Mine fault zone is characterized by chloritic breccia and mylonite with top-to-the-west shear sense (Fryxell et al., 1992; Duebendorfer and Sharp, 1998) and is estimated to have accommodated ~15 km of slip (Wernicke and Axen, 1988; Duebendorfer et al., 1998) at an average slip rate of 8.6 ± 6 km/m.y. (Fitzgerald et al., 2009).

The SVWHD is covered by Tertiary and Quaternary sediments from the southern part of Gold Butte to Lake Mead, but it is well exposed on the southern edge of Lake Mead near Salt Spring Wash, where it is referred to as the Salt Spring fault (Fig. 1). This detachment fault segment is also characterized by top-to-the-west shear sense and exhumed a thick crustal section in its footwall (Fitzgerald et al., 2009). In this paper we refer to this tilted section as the northern White Hills block. The Salt Spring fault zone consists of brecciated crystalline footwall rocks, clay-rich fault gouge, and, locally, a microbreccia ledge (Duebendorfer and Sharp, 1998; Duebendorfer et al., 2010).

The Cyclopic Mine fault is the southern continuation of the SVWHD (Fig. 1). This fault is characterized only by brittle deformation features such as breccia and gouge (Myers et al., 1986; Theodore et al., 1987), dips ~20° to the southwest (Myers et al., 1986), and displaces a Cretaceous granitic stock ~5 km westward (Theodore et al., 1987; Duebendorfer and Sharp, 1998). The slip rate on this portion of the SVWHD has been estimated at 1.2 ± 1.1 km/m.y. (from apatite fission-track [AFT] modeling; Fitzgerald et al., 2009).

Based on the apparent differences in structural styles along the SVWHD, from ductile and brittle faulting in the north to purely brittle in the south, as well as an apparent gradient in fault offset, from ~15 km across the Lakeside Mine fault to ~5 km across the Cyclopic Mine fault, Duebendorfer and Sharp (1998) proposed a southward-diminishing, along-strike exhumation gradient for the SVWHD. A large suite of AFT results suggests that exhumation was synchronous along the length of the detachment system and that this exhumation gradient results from a north-south slip rate gradient along the detachment system, rather than from variations in slip duration (Fitzgerald et al., 2009).

GEOLOGY OF THE SALT SPRING WASH AREA

To the south of Lake Mead, the Salt Spring fault is well exposed over an along-strike distance of ~5 km (Fig. 2; Duebendorfer and Sharp, 1998; Howard, 2003). The fault dips ~25° in this area and separates Proterozoic crystalline basement rocks in the footwall from Tertiary conglomerate in the hanging wall. The conglomerate, ~300 m in maximum thickness, includes debris flows, megabreccias, and intercalated volcanic rocks (Howard, 2003). A tuff within the lower part of the conglomerate has a sanidine $^{40}Ar/^{39}Ar$ age of ca. 15 Ma (Duebendorfer and Sharp, 1998), and the upper part of the conglomerate interfingers with ca. 8 Ma basalt (Howard, 2003). At the location described in the following discussion, the conglomerate dips into the Salt Spring fault at an angle of ~40° (Howard, 2003). Dips in the conglomerate shallow upsection, such that the youngest conglomerates are flat lying (Howard et al., 2010). The uppermost part of the section overlaps the fault, indicating an end to fault activity by ca. 8 Ma (Howard, 2003). At Gold Butte, Paleozoic sediments nonconformably overlying Proterozoic basement dip ~40° to the east, and Late Miocene to Pliocene sediments deposited on the SVWHD footwall are also tilted to the east, at angles of 5°–20° (Felger and Beard, 2010). These observations suggest that the fault was active at a relatively high angle and has subsequently rotated to its present moderate to low dip (Duebendorfer and Sharp, 1998; Brady et al., 2000; Fitzgerald et al., 2009; Howard et al., 2010). Slip at low angles is not necessarily precluded by the angular relationship between the fault and hanging-wall strata, however, and the fault may have an overall listric geometry. Detachments that were active at low angles have been described from other parts of the Lake Mead region (Karlstrom et al., 2010; Quigley et al., 2010).

The Miocene hanging-wall strata have been interpreted as syntectonic supradetachment basin fill derived from erosion of the exhuming footwall (Howard, 2003; Blythe et al., 2010; Howard et al., 2010; see also Friedmann et al., 1994), which consists of foliated granite and gneiss with local mylonitic zones. At our study area, the immediate footwall is the leucogranite of Greggs Hideout (Howard, 2003), which has been correlated with a 1.68 Ga monzogranite exposed to the southeast (Blacet, 1975; Chamberlain and Bowring, 1990).

The best exposure of the Salt Spring fault includes a 9-m-thick stratified zone of brecciated granite in a clay matrix (fault breccia), overlain by a relatively thin (<1 m) layer of finer grained, foliated, clay-rich fault gouge that is in direct contact with overlying Tertiary conglomerate (Figs. 3A, 3B). At this location, small-scale high-angle faults sole into a discrete band of red, foliated gouge (the principal slip zone; Figs. 3B, 3C). Foliation within the fault gouge and stratification within the fault breccia are subparallel to the dip of the fault. Overall, the structural arrangement is similar to detailed descriptions of the Death Valley turtleback faults (e.g., Hayman, 2006), where shear is focused at a principal shear plane within the relatively narrow gouge zone, dissipates downward into the brecciated zone, and ultimately reaches zero in undeformed footwall rocks (Cowan et al., 2003).

SAMPLING AND METHODS

Clay Mineralogy

We examined outcrops of the Salt Spring fault over several kilometers along strike and collected samples of gouge, fault breccia, and overlying conglomerate from two locations (Figs. 2, 3A, and 3D). These samples were crushed with a mortar and pestle, and micron- to submicron-size fractions were separated with a centrifuge. Random and oriented clay mounts were scanned with a Scintag X1 powder X-ray diffractometer at the University of Michigan. Bulk mineralogy was determined through identification of diffraction peaks from the oriented mounts (e.g., Moore and Reynolds, 1997), and detailed examination of illite polytypism was conducted on random mounts using the general procedure in Haines and van der Pluijm (2008).

AFT Thermochronology

Apatite was separated from gouge sample HM12 (the red foliated gouge shown in Figs. 3A–3C) using standard magnetic and density methods. The grains were etched with HNO_3 to reveal natural fission tracks and irradiated using a ^{252}Cf source. Fission-track ages of 38 gouge apatite grains were determined by Apatite to Zircon, Inc. (Donelick et al., 2005).

^{40}Ar/^{39}Ar Thermochronology

Muscovite

^{40}Ar/^{39}Ar laser step-heating experiments were conducted on two separate hand-picked muscovite grains from a sample of the Proterozoic leucogranite of Greggs Hideout (Howard, 2003) in the footwall of the Salt Spring fault. The sample was collected ~300 m southeast of the trace of the fault (Figs. 1 and 2). Muscovite was wrapped in pure Al foil and irradiated at the McMaster Nuclear Reactor (McMaster University, Hamilton, Ontario) in irradiation package mc26. The hornblende MMhb-1 standard (K-Ar age of 520.4 Ma; Samson and Alexander, 1987) was used as a neutron-fluence monitor. Samples were step heated with a Coherent Innova 5W continuous argon-ion laser from 0 to 4 W. Ar isotopes were measured on a VG1200S mass spectrometer, and system blanks were analyzed every five heating steps. Blank levels from Ar masses 36 through 40 were subtracted from sample gas fractions. Corrections were made for the decay of ^{37}Ar and ^{39}Ar, the production of ^{36}Ar from ^{36}Cl, and interfering nucleogenic reactions from K, Ca, and Cl.

Illite

^{40}Ar/^{39}Ar step-heating experiments were also conducted on clay-size material from three samples: two from gouge along the Salt Spring fault, and one from the fine-grained matrix of the conglomerate near the base of the supradetachment basin, ~2 m above the fault (Fig. 2). Five grain size aliquots (2–4 µm, 0.75–2 µm, 0.2–0.75 µm, <0.2 µm, and <0.05 µm equivalent spherical diameter) were made for each sample using a centrifuge. Prior to irradiation, the separates

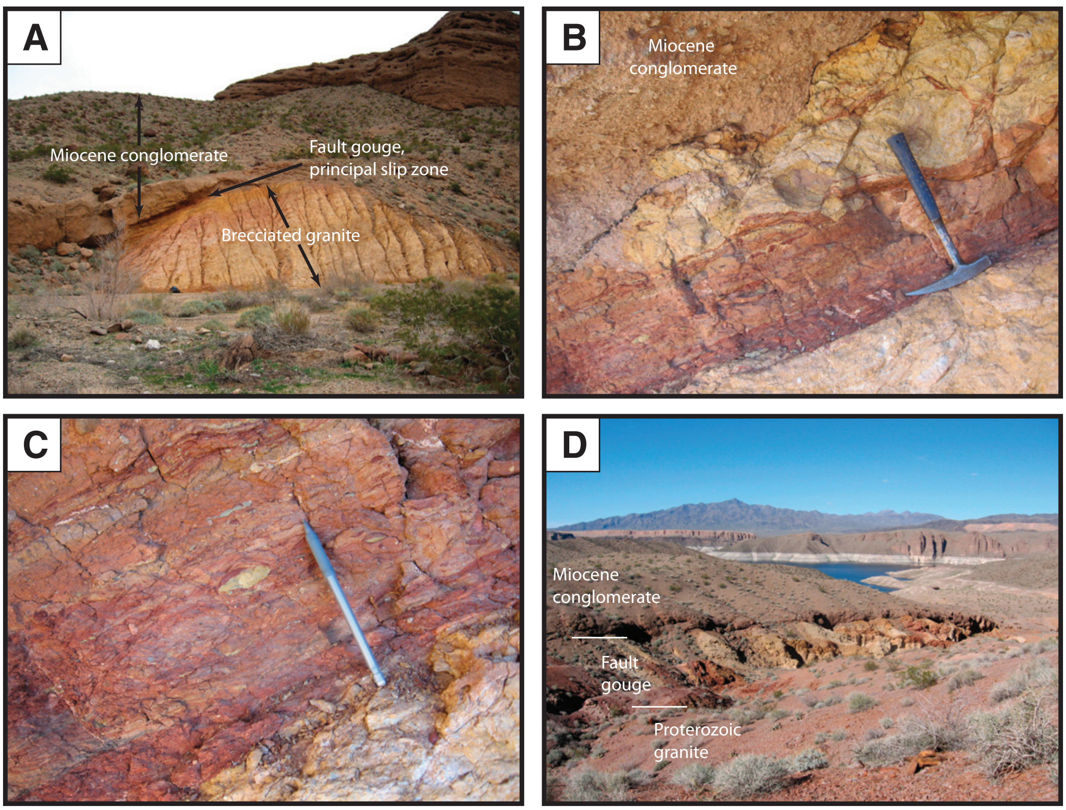

Figure 3. Photographs of the Salt Spring fault. (A) North-looking view of the stratified fault zone separating undeformed Miocene conglomerate from Proterozoic crystalline rocks. Backpack (0.5 m tall) at base of cliff for scale. (B) High-angle faults soling into a band of red fault gouge within the principal slip zone. (C) Foliated fault gouge in the principal slip plane. Sample HM12 is from the red fault gouge shown in 3B and C, and sample HM16 is from the Miocene conglomerate shown in 3A and B. (D) North-looking view of the Salt Spring fault with Gold Butte in the background. Sample HM18 is from fault gouge at this location.

were vacuum encapsulated in quartz glass tubes. Following irradiation, the tubes were broken open under vacuum, and step heating was conducted with a continuous Ar ion laser as described previously. Using the encapsulation procedure, the proportion of ^{39}Ar that is released before any heating occurs (i.e., the amount that is immediately released when the tube is broken open) can be quantified. For clays, this can be a significant fraction of the total ^{39}Ar released (e.g., Dong et al., 2000).

RESULTS

Clay Mineralogy of the Salt Spring Fault

Clay minerals are minor constituents of the Proterozoic leucogranite of Greggs Hideout in the footwall of the Salt Spring fault, but are abundant in both the supradetachment basin and fault gouge. Illite and smectite are the primary clay minerals in the conglomerate, the gouge, and the zone of brecciated granite. Illite in the gouge varies from ~5% to 55% 2M1 polytype in the various grain sizes. Illite within the Tertiary conglomerate ranges from ~10% to 30% 2M1.

AFT Data

Fission-track lengths and densities were measured from 38 apatite grains. The pooled AFT age from the gouge apatites is 15.1 ± 1.1 Ma, and the mean track length is 13.01 ± 0.26 µm.

$^{40}Ar/^{39}Ar$ Thermochronology

Muscovite

Total gas ages from 2 muscovites in the footwall sample are 876.8 ± 2.8 Ma (1σ) and 916.4 ± 2.7 Ma. Neither $^{40}Ar/^{39}Ar$ spectrum has a true plateau, although both spectra are relatively flat over most temperature steps (Fig. 4A; Supplemental Table 1[1]).

Illite

X-ray diffraction analysis indicates that illite is the primary K-bearing mineral in the micron- to submicron-scale material that was examined with $^{40}Ar/^{39}Ar$ step heating. Figure 4B shows the $^{40}Ar/^{39}Ar$ step-heating results from five grain-sizes of three samples: two samples from fault gouge and one from the matrix of Miocene conglomerate in the hanging wall of the Salt Spring fault. The $^{40}Ar/^{39}Ar$ spectra from all of these separates are staircase shaped (Fig. 4B; Supplemental Table 1 [see footnote 1]). Total gas ages decrease with decreasing grain size and vary from 5.7 to 37 Ma in the gouge samples (samples HM12 and HM18) and 12.5–65 Ma in the conglomerate (sample HM16). The maximum age from the highest temperature step of any sample is ca. 135 Ma (the 2–4 µm and 0.75–2 µm sizes from the conglomerate sample HM16). Maximum ages from gouge samples and from other sizes of the conglomerate sample are typically ca. 100 Ma or younger.

The smallest separates (<0.05 µm) released 54%–78% of their total ^{39}Ar prior to heating (Fig. 4B). The initial gas released is dominantly, if not exclusively, ^{39}Ar and therefore has an apparent age near zero. The $^{40}Ar/^{39}Ar$ spectra from the four largest grain sizes of gouge sample HM12 are nearly indistinguishable, although there is a reduction in the total gas age from 27 to 22 Ma with decreasing grain size. In contrast, the three largest aliquots of the conglomerate sample (HM16) released relatively little (24%–27%) ^{39}Ar prior to heating and have maximum ages that are older than or roughly equal to the large grain sizes of HM12. The $^{40}Ar/^{39}Ar$ spectra from gouge sample HM18 are, in many ways, intermediate between gouge sample HM12 and conglomerate sample HM16.

DISCUSSION

Exhumation Gradient along the SVWHD

The majority of thermochronology data from Gold Butte suggest that it is a tilted crustal section consisting of ~15 km of Proterozoic basement rocks nonconformably overlain by ~4 km of Phanerozoic strata (Fig. 5; Wernicke and Axen, 1988; Fryxell et al., 1992; Brady et al., 2000; Reiners et al., 2000; Bernet, 2009; Fitzgerald et al., 2009). Muscovite $^{40}Ar/^{39}Ar$ total gas ages from the basal part of this ~19-km-thick section are ca. 90 Ma, while muscovites from shallower structural positions have K-Ar and $^{40}Ar/^{39}Ar$ total gas ages of ca. 1000 Ma or older (Fig. 1; Wasserburg and Lanphere, 1965; Reiners et al., 2000). The muscovite Ar partial retention zone (PRZ), which separates structurally deep muscovites with young apparent ages from structurally shallow muscovites with old apparent ages, extends from ~9–13 km below the Phanerozoic unconformity (Reiners et al., 2000). In map view, muscovites with Ar cooling ages of ca. 90 Ma have been measured from as far as 2 km east of the Lakeside Mine fault, and the structurally deepest sample with a muscovite $^{40}Ar/^{39}Ar$ total gas age older than 100 Ma is ~8 km east of the fault (Fig. 1; Reiners et al., 2000).

Muscovite from our footwall sample of the northern White Hills block, located ~300 m from the Salt Spring fault, yields an apparent age of ca. 900 Ma (Fig. 4). Duebendorfer and Sharp (1998) conducted $^{40}Ar/^{39}Ar$ step-heating analysis of muscovite from a mylonitic leucogranite located a similar distance from the fault, but to the southwest of our sample location and at a structurally deeper position. Their muscovite had a total gas age of 372 Ma, a complex $^{40}Ar/^{39}Ar$ spectrum (possibly related to mylonitization and multiple periods of heating and cooling), and maximum ages during step heating of ca. 550 Ma (see Fig. 14 of Duebendorfer and Sharp, 1998). Our new sample is nonmylonitized and produced much simpler step-heating spectra (Fig. 4). Both samples have total gas ages that are intermediate in the range of muscovite ages at Gold Butte, although muscovite grains from our sample have ages (ca. 900 Ma) much closer to muscovite ages from structurally shallow parts of Gold Butte. We interpret both our result and the previous result from Duebendorfer and Sharp (1998) as evidence that the northern White Hills samples are within the fossil muscovite Ar PRZ. The age of our new sample suggests that it is in the upper part of the PRZ and was previously at a paleodepth of ~14 km, based on comparison with thermochronology data from Gold Butte.

The Phanerozoic cover of the northern White Hills section is not preserved and is believed to have been eroded off of basement exposures during Late Cretaceous–early Tertiary formation of the Kingman arch (Bohannon, 1984; Faulds et al., 2001). We assume that the Phanerozoic section in the northern White Hills was originally of similar thickness (~4 km) to that at Gold Butte, suggesting that our muscovite sample location was ~10 km below the Phanerozoic unconformity prior to late Mesozoic through Cenozoic exhumation. In contrast, the base of the currently exposed Gold Butte crustal section was ~15 km below the same unconformity (Fig. 5; Fryxell et al., 1992; Fitzgerald et al., 2009). There are currently no muscovite Ar data available from near the Cyclopic detachment, which is a key location for testing the hypothesis of an overall north to south decrease in exhumation along the SVWHD. Nevertheless, from the existing muscovite Ar data described here, it is clear that the locations of our sample and the sample of Duebendorfer and Sharp (1998) are at structurally shallower positions than the base of the Gold Butte block, consistent with a north to south decrease in exhumation magnitude (Fitzgerald et al., 2009). Furthermore, our new data from near the Salt Spring fault imply that footwall locations immediately to

[1]Supplemental Table 1. Excel file of $^{40}Ar/^{39}Ar$ step-heating results. If you are viewing the PDF of this paper or reading it offline, please visit http://dx.doi.org/10.1130/GES00616.S1 or the full-text article on www.gsapubs.org to view Supplemental Table 1.

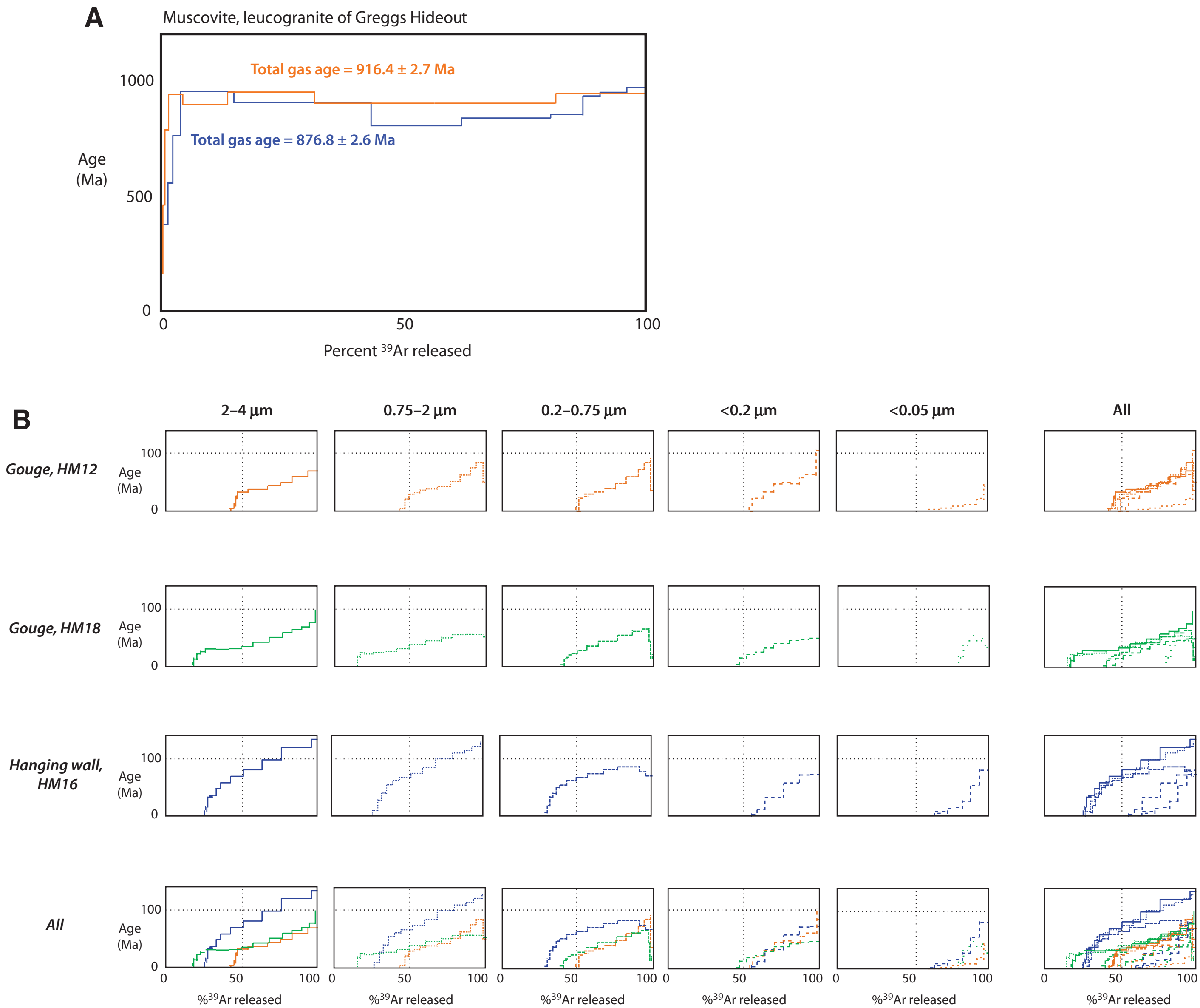

Figure 4. $^{40}Ar/^{39}Ar$ step-heating spectra from (A) muscovite and (B) illite.

the east of the fault (updip) have muscovite Ar ages older than 900 Ma. As explained in a subsequent section, the apparent restriction of muscovite with Cretaceous apparent ages to Gold Butte can be exploited to investigate the provenance of muscovite within the Miocene supradetachment basin.

Clay-Rich Fault Gouge

Slip on low-angle detachment faults, and whether movement along these faults is dominantly seismic or aseismic, are long-standing issues in structural geology. Clay-rich fault gouge is a factor in this debate because (1) low frictional coefficients typical of clays may permit slip on detachment faults at low angles (Numelin et al., 2007), and (2) recent experiments suggest that some clays promote creep instead of seismic slip (Ikari et al., 2009). Although it is not clear if the Salt Spring fault was active at a low angle, similarities with the Death Valley turtleback faults suggest that the Salt Spring fault may be typical of the shallow segments of detachment faults. The primary clays within gouge along the Salt Spring fault are illite and smectite. These low-frictional-coefficient, velocity-strengthening clay minerals are particularly impermeable when sheared and will have elevated pore pressures and reduced shear strength in the presence of fluids (Ikari et al., 2009).

It has been shown in some cases that the clay mineralogy of fault gouge differs from the clay mineralogy of adjacent wall rocks (Fig. 6A; Vrolijk and van der Pluijm, 1999), suggesting that authigenic mineral growth within fault zones may be an important factor influencing the mechanical behavior of faults. However, similarities in clay mineralogy between gouge and hanging-wall conglomerate at our study locality suggest that authigenic mineral growth within the fault zone is not the case along the Salt Spring fault. Samples from the matrix of the conglomerate contain illite and smectite, similar to the fault gouge, and detailed illite polytype compositions are comparable between clay in the conglomerate and clay in the fault gouge

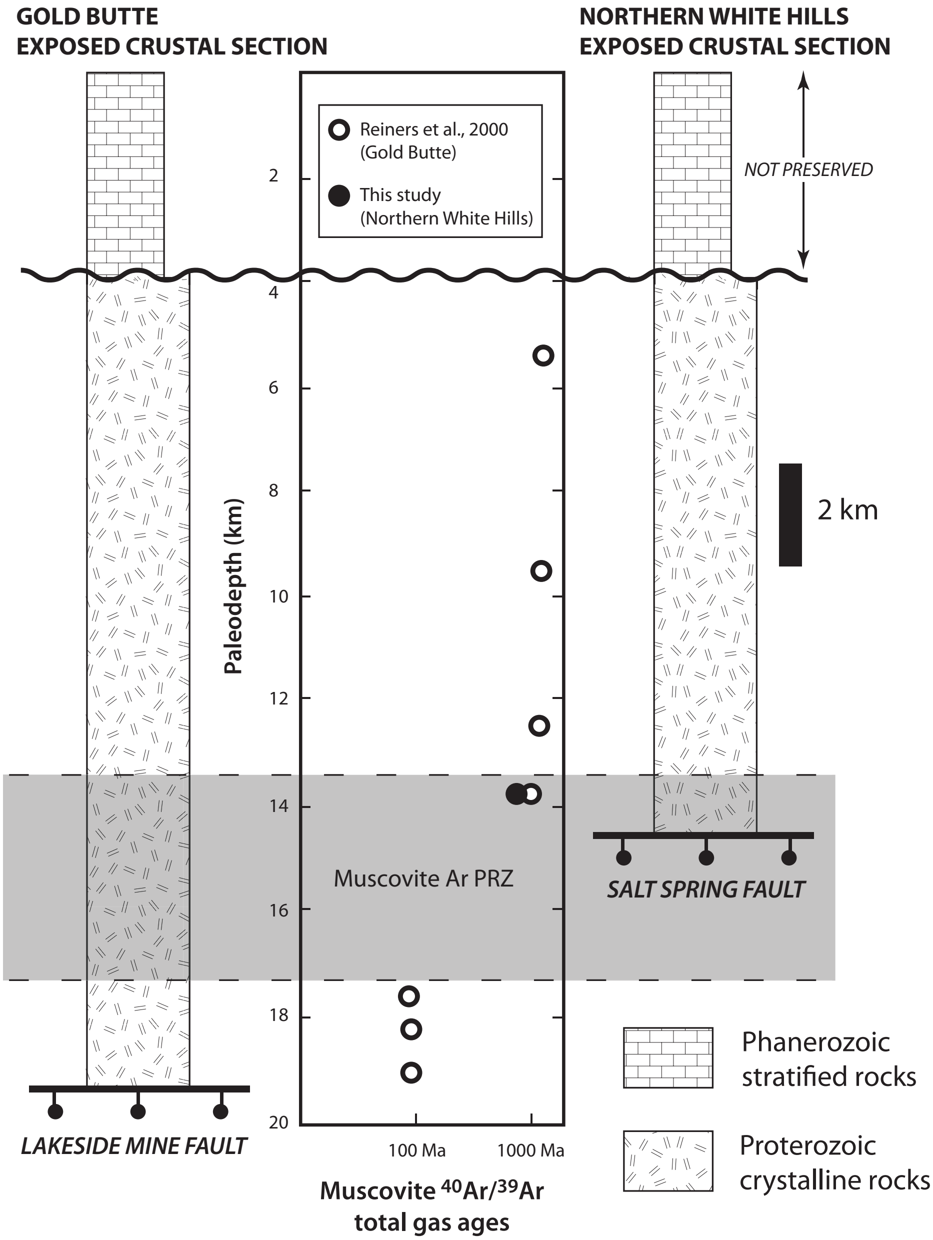

Figure 5. Geologic sections of Gold Butte and the northern White Hills, showing presumed depth of exposure relative to the sub-Phanerozoic unconformity. Phanerozoic strata are preserved at Gold Butte but were eroded from the White Hills during formation of the Kingman arch (Bohannon, 1984). Thickness of Phanerozoic strata at the northern White Hills is assumed to have been similar to that preserved at Gold Butte. PRZ—partial retention zone.

(Fig. 6B). The fault is in direct contact with the conglomerate (Fig. 3), so a reasonable inference is that clay minerals within the fault gouge were scraped from the base of the hanging-wall strata. Clasts from the conglomerate were likely comminuted through mechanical abrasion when they were incorporated into the principal slip zone of the fault. Clay mineral compositions are sensitive to temperature (e.g., Hunziker et al., 1986), and the fact that clays within exposures of the Salt Spring fault were not transformed to higher temperature compositions than adjacent wall rocks suggests that any fluids that may have circulated within the fault were at relatively low temperature, as documented further with AFT data. These findings imply that the presence of clay-rich gouge and its attendant effects on fault strength at shallow levels are controlled, in large part, by the composition of rocks in contact with faults. At the exposures we studied, clays in gouge were derived from a relatively thin (~300 m) syntectonic formation, although clay-rich gouge could also be present within deeper portions of the fault.

Source of Detrital Illite-Muscovite in the Supradetachment Basin

Illite in sedimentary rocks can be detrital or authigenic. Detrital illite is very fine-grained muscovite derived from an igneous or metamorphic source. In low-grade shales (e.g., diagenetic grade or zeolite facies), detrital illite-muscovite is generally more Ar retentive than authigenic illite (Dong et al., 2000). Staircase-shaped $^{40}Ar/^{39}Ar$ spectra are often produced during step-heating experiments of these particularly low-grade shales and seem to arise from the mixing of retentive, detrital illite-muscovite with less retentive authigenic illite. Clay-size separates from very low grade shales also lose significant amounts of ^{39}Ar during irradiation (Dong et al., 2000). At higher metamorphic grade (e.g., anchizone-epizone), authigenic illite grains are thicker (e.g., Merriman et al., 1990; Jiang et al., 1997; Jaboyedoff and Cosca, 1999), $^{40}Ar/^{39}Ar$ spectra are frequently flatter (Hunziker et al., 1986), and there is less ^{39}Ar loss during irradiation (Dong et al., 1995, 2000).

The $^{40}Ar/^{39}Ar$ and clay mineralogy data from micron to submicron grain sizes of the matrix of the Miocene conglomerate in the northern White Hills have all of the main characteristics of very low grade sediments: abundant smectite and 1Md illite, staircase-shaped $^{40}Ar/^{39}Ar$ spectra, and significant (12%–78%) loss of ^{39}Ar during irradiation. We suggest that these spectra result from the mixing of relatively large, retentive, detrital illite-muscovite derived from Proterozoic crystalline rocks with smaller, less retentive, authigenic illite. In that case, two parameters are meaningful in interpreting illite $^{40}Ar/^{39}Ar$ data from our samples: the amount of ^{39}Ar expelled during irradiation (i.e., the proportion of ^{39}Ar that is released when the encapsulating tubes are initially broken open) and the maximum ages measured during step heating. The ^{39}Ar loss during irradiation is an indicator of ^{40}Ar retention in nature (Dong et al., 1995), and maximum step-heating ages can reflect the apparent ages of detrital muscovite in very low grade sediments (Dong et al., 2000). Maximum ages from the step-heating spectra of the conglomerate sample (HM16) range from 75 to 135 Ma and are correlated with grain size (Fig. 4). Our interpretation is that the most retentive detrital grains having the oldest apparent ages are concentrated in the

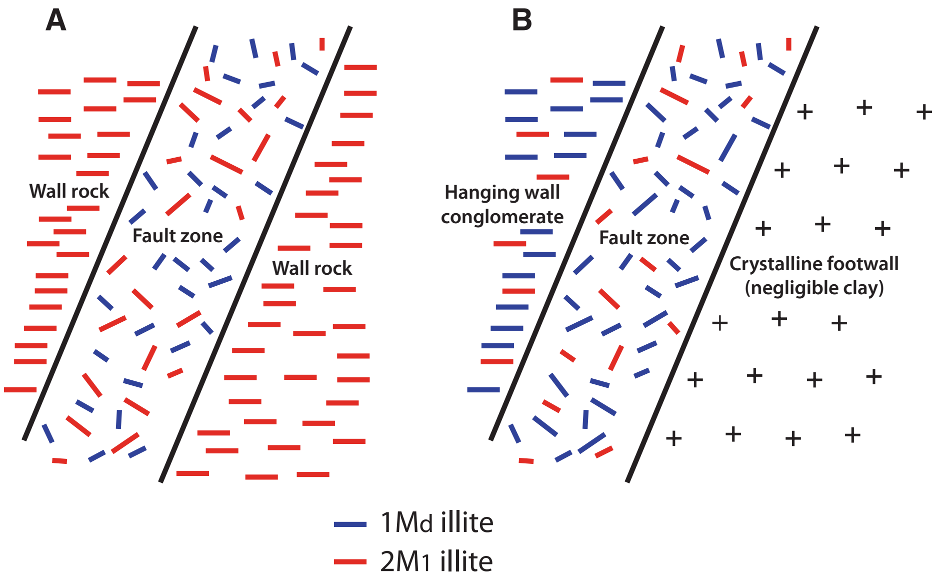

Figure 6. Illite polytype composition of fault zones. (A) Model for unique growth of 1Md illite polytype in fault zones (Haines and van der Pluijm, 2008). (B) Diagram more appropriate to the Salt Spring fault, illustrating that both the hanging wall conglomerate and fault gouge are composed of ~70% 1Md illite.

largest size fractions and are less abundant in smaller sizes. As a result, larger size fractions generally have older maximum ages and less ^{39}Ar loss during irradiation. This interpretation implies that the maximum age from the coarsest size fraction (ca. 135 Ma) is our best estimate for the apparent age of detrital illite in the Miocene conglomerate.

The ^{40}Ar/^{39}Ar spectra from the gouge samples are also staircase shaped and are marked by significant ^{39}Ar loss during irradiation. Maximum ages from these spectra are 46–106 Ma, broadly similar to, but somewhat younger than, maximum ages from the adjacent hanging wall. Because spectra from gouge sample HM18 are intermediate between those from the conglomerate sample and the other gouge sample, we concentrate on the two primary differences between the results from hanging-wall sample HM16 and gouge sample HM12: relatively coarse sizes from HM16 lost less ^{39}Ar during irradiation than HM12, and maximum ages from large sizes during step heating are older in HM16 than in HM12 (Fig. 4). We envision three potential explanations for this difference. First, the fault gouge samples could include relatively young illite that formed in the fault zone but not in the adjacent hanging wall, a scenario that has been proposed for other faults (e.g., Vrolijk and van der Pluijm, 1999; van der Pluijm et al., 2001; Solum et al., 2005; Haines and van der Pluijm, 2008). Second, illite within the gouge samples may be particularly Ar unretentive. A potential explanation for our data is that mechanical deformation of illite grains within the fault gouge has created micron- to submicron-scale defects and dislocations that are conduits for Ar loss, as has been proposed for deformed muscovite grains in ductile shear zones (Mulch et al., 2002). Third, fault zone heating could have partially degassed illite within fault gouge, leading to younger illite ^{40}Ar/^{39}Ar ages in the fault zone than in adjacent wall rocks. Although this alternative is a potential explanation for younger ^{40}Ar/^{39}Ar ages in general, it is not clear that this process alone could account for greater ^{39}Ar loss during irradiation in the gouge samples.

The primary observation from these data is that there is no indication of detrital muscovite with an apparent age of ca. 900 Ma or older, the age of footwall muscovite directly updip of our sample location. The most likely nearby source for ca. 135 Ma muscovite is Gold Butte, which we suggest formed a Miocene upland area that shed detritus southward into the supradetachment basin (Fig. 7). Detrital muscovite and/or illite with a maximum apparent age of ca. 135 Ma, sourced from Gold Butte, are now found in the basin at least as far south as the southern edge of Lake Mead, where we sampled them. Where cut by the Salt Spring fault, these detrital grains were incorporated into clay-rich fault gouge.

Clast composition of the Miocene conglomerate at our sample location is consistent with derivation from Gold Butte (Howard et al., 2010), though the majority of paleocurrent data from the conglomerate near the Salt Spring fault suggest source regions to the east and southeast (Blythe et al., 2010). Paleocurrent data from the western part of the basin are generally southwest directed, however, reflecting Middle Miocene development of a drainage system with headwaters in the vicinity of Gold Butte (Blythe et al., 2010). Our new data suggest that this system was the dominant source of detrital material in the supradetachment basin, even in eastern locations near the Salt Spring fault.

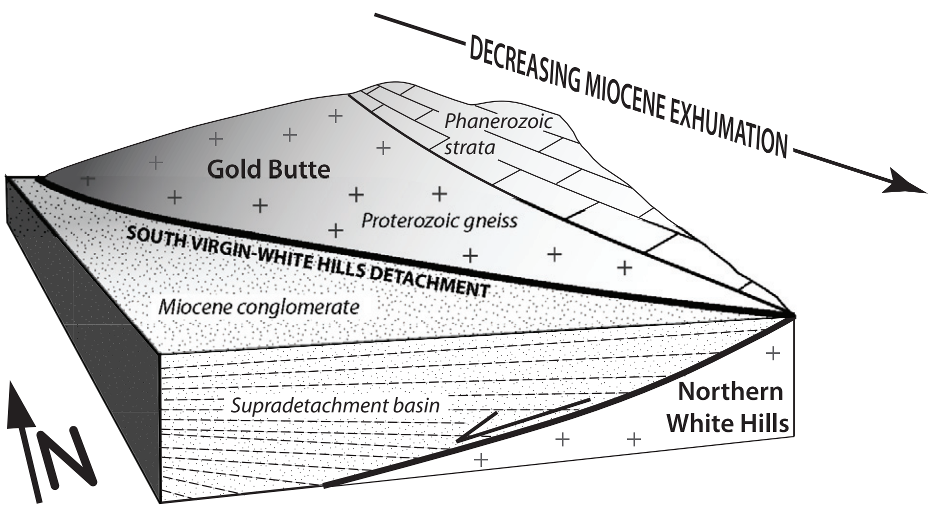

Figure 7. Block diagram showing evolution of the Gold Butte block and Salt Spring supradetachment basin. During Miocene time Gold Butte formed an eroding upland area that shed detritus into the supradetachment basin to the south.

Pressure and Temperature Conditions of the Salt Spring Fault Gouge

Our interpretation that gouge along the Salt Spring fault formed principally by scraping clay from the syntectonic hanging-wall conglomerate implies that the stratigraphic thickness of the conglomerate places limits on the depth at which the gouge formed. The maximum thickness of the conglomerate is ~300 m (Howard, 2003), corresponding to a lithostatic stress of ~6 MPa (using a density of 2 g/cm^3 for unconsolidated sediment), which we suggest is a reasonable upper bound for formation of gouge in this location. Laboratory experiments on clay fabrics produced under different conditions of normal stress and shear strain indicate that the weak fabrics typically exhibited by gouge can be generated with normal stresses of 5–25 MPa, lending support to our conclusion (Haines et al., 2009).

The same low-temperature thermochronology techniques that have been used to investigate the exhumation of detachment footwalls can also be used to reconstruct thermal histories of fault rocks (Tagami et al., 1988; Omar et al., 1994; d'Alessio et al., 2003; Tagami, 2005). Our fission-track data from apatites entrained in the Salt Spring fault, when compared with AFT data from the crystalline footwall, show no indication of a thermal overprint that could be ascribed to their position within the fault. Apatite grains in the gouge have a mean fission-track age of 15.1 ± 1.1 Ma and a mean track length of 13.01 ± 0.26 µm. For comparison, six previously reported fission-track ages from the footwall of the Salt Spring fault range in age from 12.6 ± 1.8 to 18.5 ± 1.7 Ma and have mean track lengths that vary from 13.2 ± 0.2 to 14.6 ± 0.1 µm (Fitzgerald et al., 2009). AFT ages from structurally deep parts of the Gold Butte block are ca. 11–16 Ma, and average ca. 15 Ma (Fitzgerald et al., 1991, 2009). Given the other available provenance constraints on the source of basin fill in the Salt Spring region, it is most likely that apatites in the gouge were scraped from the hanging wall of the Salt Spring fault and were ultimately sourced from Gold Butte, although the observed AFT ages do not preclude a local provenance. The similarity in AFT ages and track-length distributions from the fault gouge to those observed in bedrock samples would suggest that at the paleodepth (≤~300 m) of our sample, (1) shear heating had no measurable effect on AFT lengths or densities, and (2) either there were no fluids flowing along the fault, or the fluids were not hot enough, or of sufficient duration, to measurably alter fission-track ages or length distributions of apatite grains within the gouge.

The conglomerate in the hanging wall at our sample location is from the lower part of the Miocene supradetachment basin and is correlative with a section containing a 12 Ma tuff (Howard, 2003). This part of the conglomerate is cut by the fault, so the AFT age of ca. 15 Ma is older than the most recent activity on the fault. This indicates that the AFT ages were not completely reset by virtue of frictional or hydrothermal heating along the fault. Abundant low-temperature clays within the gouge (smectite and 1Md illite) support the conclusion that the fault gouge did not experience elevated temperature, consistent with previous observations of gouge from the Death Valley turtleback faults (Hayman, 2006).

Our thermochronology data also suggest that ~3 m.y. elapsed between the time the gouge apatites cooled through the AFT partial annealing zone and the time they were deposited in the supradetachment basin. This lag time corresponds with an exhumation rate, which can be compared with the exhumation rate gradient along the SVWHD. For a geothermal gradient of 20 °C (Reiners et al., 2000), an AFT effective closure temperature of 120 °C, and a lag time of 3 m.y., the minimum exhumation rate of the gouge apatites was 2 km/m.y. This is a minimum estimate because (1) the apatites could have spent some time at the surface after being exhumed but before being eroded, (2) a significant amount of time could have elapsed between erosion of the apatites from a crystalline source and final deposition in the basin, and (3) the apatites could have been incorporated into gouge from stratigraphically deeper parts of the conglomerate. For a normal fault dipping 60° (the estimated original dip of the SVWHD; Wernicke and Axen, 1988; Fitzgerald et al., 2009), a minimum exhumation rate of 2 km/m.y. corresponds with a minimum fault slip rate of 2.3 km/m.y. Fault slip rates based on AFT data decrease southward along the SVWHD from 8.6 ± 6 km/m.y. at the Lakeside Mine fault to 1.2 ± 1.1 km/m.y. at the Cyclopic Mine fault (Fitzgerald et al., 2009). While acknowledging that the exhumation rate calculation is based on assumed values for several key parameters, our estimate is consistent with a north to south decrease in exhumation along the SVWHD, and suggests that much of this decrease occurs between the Lakeside Mine fault and the Salt Spring fault.

CONCLUSIONS

The Salt Spring fault in northernmost Arizona forms the central segment of the SVWHD and separates Proterozoic crystalline rocks in its footwall from Miocene conglomerate in its hanging wall. The clay mineral composition of gouge from the Salt Spring fault is similar to the matrix of adjacent Miocene conglomerate, suggesting that fault gouge clay minerals were derived from the conglomerate. Apatite grains entrained in the gouge have fission-track ages and track-length distributions that are similar to those of footwall apatites, indicating that insufficient heat was generated through shear heating or circulation of fault fluids to reset fault gouge AFT ages. Apatite grains entrained in the gouge have a history consisting of (1) crystallization within Proterozoic basement rocks, (2) exhumation in the footwall of the SVWHD, (3) erosion and deposition into the hanging-wall supradetachment basin, and (4) incorporation into the fault zone along with abundant clay minerals.

The $^{40}Ar/^{39}Ar$ results from clay in the fault gouge are also similar to results from the matrix of the conglomerate. Maximum ages from the largest sizes of conglomerate $^{40}Ar/^{39}Ar$ spectra are ca. 135 Ma, which we suggest is the apparent age of detrital muscovite in the conglomerate. At our footwall sample location (and presumably farther updip), muscovite $^{40}Ar/^{39}Ar$ ages are ca. 900 Ma or older. The most likely source for ca. 135 Ma detrital muscovite in the Miocene basin is Gold Butte, located 20 km to the north. Erosion of the exhumed Gold Butte block shed detritus southward into the supradetachment basin (Fig. 7), and these materials were subsequently scraped out of the basin and incorporated into the Salt Spring fault. AFT and illite $^{40}Ar/^{39}Ar$ results from the Salt Spring fault thus reflect the thermal history of the Gold Butte crustal section, and not the thermal evolution of the immediately adjacent footwall of the Salt Spring fault.

Our new results are consistent with a southward-diminishing exhumation gradient along the SVWHD. Gold Butte exposes structural levels below the muscovite $^{40}Ar/^{39}Ar$ PRZ, in contrast to the northern White Hills block, located along the central portion of the SVWHD, which is exposed only to the depth of the upper part of the PRZ. The present-day exhumation pattern is the reverse of the southward-increasing denudation gradient established during Late Cretaceous–early Tertiary formation of the Kingman arch and reflects variation in the magnitude of Miocene extension across the SVWHD.

ACKNOWLEDGMENTS

We thank Chris Hall for measuring $^{40}Ar/^{39}Ar$ ages, Paul O'Sullivan for conducting the fission-track analyses, and Anthony Monatesti for scientific permits to the Lake Mead National Recreation Area. Constructive reviews by Gary Axen and Mark Quigley improved the paper. This research was supported by National Science Foundation grant EAR-0738435 and postdoctoral funds from the University of Michigan.

REFERENCES CITED

Anderson, E.M., 1942, The dynamics of faulting and dyke formation with application to Britain: Edinburgh, Scotland, Oliver and Boyd, 191 p.

Anderson, R.E., 1971, Thin-skin distension in Tertiary rocks of southwestern Nevada: Geological Society of America Bulletin, v. 82, p. 43–58, doi: 10.1130/0016-7606(1971)82[43:TSDITR]2.0.CO;2.

Anderson, R.E., and Beard, L.S., 2010, Geology of the Lake Mead region: An overview, *in* Umhoefer, P.J., et al., eds., Miocene tectonics of the Lake Mead region, central Basin and Range: Geological Society of America Special Paper 463, p. 1–28, doi: 10.1130/2010.2463(01).

Armstrong, R.L., 1972, Low-angle (denudation) faults, hinterland of the Sevier orogenic belt, eastern Nevada and western Utah: Geological Society of America Bulletin, v. 83, p. 1729–1754, doi: 10.1130/0016-7606(1972)83[1729:LDFHOT]2.0.CO;2.

Armstrong, R.L., 1982, Cordilleran metamorphic core complexes—From Arizona to southern California: Annual Review of Earth and Planetary Sciences, v. 10, p. 129–154, doi: 10.1146/annurev.ea.10.050182.001021.

Axen, G.J., 1992, Pore pressure, stress increase, and fault weakening in low-angle normal faulting: Journal of Geophysical Research, v. 97, p. 8979–8991, doi: 10.1029/92JB00517.

Axen, G.J., and Selverstone, J., 1994, Stress state and fluid-pressure level along the Whipple detachment fault, California: Geology, v. 22, p. 835–838, doi: 10.1130/0091-7613(1994)022<0835:SSAFPL>2.3.CO;2.

Bernet, M., 2009, A field-based estimate of the zircon fission-track closure temperature: Chemical Geology, v. 259, p. 181–189, doi: 10.1016/j.chemgeo.2008.10.043.

Blacet, P.M., 1975, Preliminary geologic map of the Garnet Mountain quadrangle, Mohave County, Arizona: U.S. Geological Survey Open-File Report 75-93, scale 1:48000.

Blythe, N., Umhoefer, P.J., Duebendorfer, E.M., McIntosh, W.C., and Peters, L., 2010, Development of the Salt Spring Wash Basin in a reentrant in the hanging wall of the South Virgin–White Hills detachment fault, Lake Mead domain, northwest Arizona, *in* Umhoefer, P.J., et al., eds., Miocene tectonics of the Lake Mead region, central Basin and Range: Geological Society of America Special Paper 463, p. 61–85, doi: 10.1130/2010.2463(04).

Bohannon, R.G., 1984, Nonmarine sedimentary rocks of Tertiary age in the Lake Mead region, southeastern Nevada and northwestern Arizona: U.S. Geological Survey Professional Paper 1259, 72 p.

Boulton, C., Davies, T., and McSaveney, M., 2009, The frictional strength of granular fault gouge; application of theory to the mechanics of low-angle normal faults, *in* Ring, U., and Wernicke, B., eds., Extending a continent; architecture, rheology and heat budget: Geological Society of London Special Publication 321, p. 9–31, doi: 10.1144/SP321.2.

Brady, R.J., 2002, Very high slip rates on continental extensional faults: New evidence from (U-Th)/He thermochronometry of the Buckskin Mountains, Arizona: Earth and Planetary Science Letters, v. 197, p. 95–104, doi: 10.1016/S0012-821X(02)00460-0.

Brady, R., Wernicke, B., and Fryxell, J., 2000, Kinematic evolution of a large-offset continental normal fault system, South Virgin Mountains, Nevada: Geological Society of America Bulletin, v. 112, p. 1375–1397, doi: 10.1130/0016-7606(2000)112<1375:KEOALO>2.0.CO;2.

Chamberlain, K.R., and Bowring, S.A., 1990, Proterozoic geochronology and isotopic boundary in NW Arizona: Journal of Geology, v. 98, p. 399–416, doi: 10.1086/629412.

Cowan, D.S., Cladouhos, T.T., and Morgan, J.K., 2003, Structural geology and kinematic history of rocks formed along low-angle normal faults, Death Valley, California: Geological Society of America Bulletin, v. 115, p. 1230–1248, doi: 10.1130/B25245.1.

Crittenden, M.D., Jr., Coney, P.J., and Davis, G.H., eds., 1980, Cordilleran metamorphic core complexes: Geological Society of America Memoir 153, 490 p.

d'Alessio, M.A., Blythe, A.E., and Bürgmann, R., 2003, No frictional heat along the San Gabriel fault, California: Evidence from fission-track thermochronology: Geology, v. 31, p. 541–544, doi: 10.1130/0091-7613(2003)031<0541:NFHATS>2.0.CO;2.

Davis, G.H., 1983, Shear-zone model for the origin of metamorphic core complexes: Geology, v. 11, p. 342–347, doi: 10.1130/0091-7613(1983)11<342:SMFTOO>2.0.CO;2.

Donelick, R.A., O'Sullivan, P.B., and Ketcham, R.A., 2005, Apatite fission-track analysis, *in* Reiners, P.W., and Ehlers, T.A., eds., Low-temperature thermochronology: Techniques, interpretations, and applications: Reviews in Mineralogy and Geochemistry Volume 58, p. 49–94, doi: 10.2138/rmg.2005.58.3.

Dong, H., Hall, C.M., Peacor, D.R., and Halliday, A.N., 1995, Mechanisms of argon retention in clays revealed by laser ^{40}Ar-^{39}Ar dating: Science, v. 267, p. 355–359, doi: 10.1126/science.267.5196.355.

Dong, H., Hall, C.M., Peacor, D.R., Halliday, A.N., and Pevear, D.R., 2000, Thermal ^{40}Ar/^{39}Ar separation of diagenetic from detrital illitic clays in Gulf Coast shales: Earth and Planetary Science Letters, v. 175, p. 309–325, doi: 10.1016/S0012-821X(99)00294-0.

Duebendorfer, E.M., and Sharp, W.D., 1998, Variation in displacement along strike of the South Virgin–White Hills detachment fault: Perspectives from the northern White Hills, northwestern Arizona: Geological Society of America Bulletin, v. 110, p. 1574–1589, doi: 10.1130/0016-7606(1998)110<1574:VIDASO>2.3.CO;2.

Duebendorfer, E.M., Beard, L.S., and Smith, E.I., 1998, Restoration of Tertiary deformation in the Lake Mead region, southern Nevada, *in* Faulds, J., and Stewart, J., eds., Accommodation zones and transfer zones: The regional segmentation of the Basin and Range province: Geological Society of America Special Paper 323, p. 127–148, doi: 10.1130/0-8137-2323-X.127.

Duebendorfer, E.M., Faulds, J.E., and Fryxell, J.E., 2010, The South Virgin–White Hills detachment fault, southeastern Nevada and northwestern Arizona: Significance, displacement gradient, and corrugation formation, *in* Umhoefer, P.J., et al., eds., Miocene tectonics of the Lake Mead region, central Basin and Range: Geological Society of America Special Paper 463, p. 275–287, doi: 10.1130/2010.2463(12).

Faulds, J.E., Feuerbach, D.L., Miller, C.F., and Smith, E.I., 2001, Cenozoic evolution of the northern Colorado River extensional corridor, southern Nevada and northwest Arizona, *in* Erskine, M.C., et al., eds., The geologic transition, high plateaus to Great Basin—A symposium and field guide: The Mackin Volume: Utah Geological Association Publication 30, p. 239–271.

Felger, T.J., and Beard, L.S., 2010, Geologic map of Lake Mead and surrounding regions, southern Nevada, southwestern Utah, and northwestern Arizona, *in* Umhoefer, P.J., et al., eds., Miocene tectonics of the Lake Mead region, central Basin and Range: Geological Society of America Special Paper 463, p. 29–38, doi: 10.1130/2010.2463(02).

Fitzgerald, P.G., Fryxell, J.E., and Wernicke, B.P., 1991, Miocene crustal extension and uplift in southeastern Nevada: Constraints from fission track analysis: Geology, v. 19, p. 1013–1016, doi: 10.1130/0091-7613(1991)019<1013:MCEAUI>2.3.CO;2.

Fitzgerald, P.G., Duebendorfer, E.M., Faulds, J.E., and O'Sullivan, P., 2009, South Virgin–White Hills detachment fault system of SE Nevada and NW Arizona: Applying fission track thermochronology to constrain the tectonic evolution of a major continental detachment fault: Tectonics, v. 28, TC2001, doi: 10.1029/2007TC002194.

Foster, D.A., Gleadow, J.W., Reynolds, S.J., and Fitzgerald, P.G., 1993, Denudation of metamorphic core complexes and the reconstruction of the transition zone, west-central Arizona: Constraints from apatite fission track thermochronology: Journal of Geophysical Research, v. 98, p. 2167–2185, doi: 10.1029/92JB02407.

Fricke, H.C., Wickham, S.M., and O'Neil, J.R., 1992, Oxygen and hydrogen isotope evidence for meteoric water infiltration during mylonitization and uplift in the Ruby Mountains–East Humboldt Range core complex, Nevada: Contributions to Mineralogy and Petrology, v. 111, p. 203–221, doi: 10.1007/BF00348952.

Friedmann, S.J., Davis, G.A., Fowler, T.K., Brudos, T., Parke, M., Burbank, D.W., and Burchfiel, B.C., 1994, Stratigraphy and gravity-slide elements of a Miocene supradetachment basin, Shadow Valley, East Mojave Desert, *in* McGill, S.F., and Ross, T.M., eds., Geological investigations of an active margin: Geological Society of America Cordilleran Section guidebook: Redlands, California, San Bernardino County Museum Association, p. 302–318.

Fryxell, J.E., Salton, G.G., Selverstone, J., and Wernicke, B., 1992, Gold Butte crustal section, South Virgin Mountains, Nevada: Tectonics, v. 11, p. 1099–1120, doi: 10.1029/92TC00457.

Glazner, A.F., and Bartley, J.M., 1991, Volume loss, fluid-flow and state of strain in extensional mylonites from the central Mojave Desert, California: Journal of Structural Geology, v. 13, p. 587–594, doi: 10.1016/0191-8141(91)90045-K.

Haines, S.H., and van der Pluijm, B.A., 2008, Clay quantification and Ar-Ar dating of synthetic and natural gouge: Application to the Miocene Sierra Mazatán detachment fault, Sonora, Mexico: Journal of Structural Geology, v. 30, p. 525–538, doi: 10.1016/j.jsg.2007.11.012.

Haines, S.H., van der Pluijm, B.A., Ikari, M.J., Saffer, D.M., and Marone, C., 2009, Clay fabric intensity in natural and artificial fault gouges: Implications for brittle fault zone processes and sedimentary basin clay fabric evolution: Journal of Geophysical Research, v. 114, B05406, doi: 10.1029/2008JB005866.

Hamilton, W., and Myers, W.B., 1966, Cenozoic tectonics of the western United States: Reviews of Geophysics, v. 4, p. 509–549, doi: 10.1029/RG004i004p00509.

Hayman, N., 2006, Shallow crustal fault rocks from the Black Mountain detachments, Death Valley, CA: Journal of Structural Geology, v. 28, p. 1767–1784, doi: 10.1016/j.jsg.2006.06.017.

Healy, D., 2009, Anisotropy, pore fluid pressure and low angle normal faults: Journal of Structural Geology, v. 31, p. 561–574, doi: 10.1016/j.jsg.2009.03.001.

Hoisch, T.D., and Simpson, C., 1993, Rise and tilt of metamorphic rocks in the lower plate of a detachment fault in the Funeral Mountains, Death Valley, California: Journal of Geophysical Research, v. 98, p. 6805–6827, doi: 10.1029/92JB02411.

Holm, D.K., and Dokka, R.K., 1993, Interpretation and tectonic implications of cooling histories: An example from the Black Mountains, Death Valley extended terrane, California: Earth and Planetary Science Letters, v. 116, p. 63–80, doi: 10.1016/0012-821X(93)90045-B.

Howard, K.A., 2003, Geologic map of the Hiller Mountains quadrangle, Clark County, Nevada, and Mohave County, Arizona: Nevada Bureau of Mines and Geology, scale 1:24000.

Howard, K.A., Beard, L.S., Kuntz, M.A., Kunk, M.J., Sarna-Wojcicki, A.M., Perkins, M.E., and Lucchitta, I., 2010, Erosion of tilted fault blocks and deposition of coarse sediments in half-graben basins during late stages of extension: Gold Butte area, Basin and Range Province, *in* Umhoefer, P.J., et al., eds., Miocene tectonics of the Lake Mead region, central Basin and Range: Geological Society of America Special Paper 463, p. 147–170, doi: 10.1130/2010.2463(07).

Hunziker, J.C., Frey, M., Clauer, N., Dallmeyer, R.D., Friedrichsen, H., Flehmig, W., Hochstrasser, K., Roggwiler, P., and Schwander, H., 1986, The evolution of illite to muscovite: Mineralogical and isotopic data from the Glarus Alps, Switzerland: Contributions to Mineralogy and Petrology, v. 92, p. 157–180, doi: 10.1007/BF00375291.

Hurlow, H.A., Snoke, A.W., and Hodges, K.V., 1991, Temperature and pressure of mylonitization in a Tertiary extensional shear zone, Ruby Mountains–East Humboldt Range, Nevada: Tectonic implications: Geology, v. 19, p. 82–86, doi: 10.1130/0091-7613(1991)019<0082:TAPOMI>2.3.CO;2.

Ikari, M.J., Saffer, D.M., and Marone, C., 2009, Frictional and hydrologic properties of clay-rich fault gouge: Journal of Geophysical Research, v. 114, B05409, doi: 10.1029/2008JB006089.

Jaboyedoff, M., and Cosca, M.A., 1999, Dating incipient metamorphism using ^{40}Ar/^{39}Ar geochronology and XRD modeling: A case study from the Swiss Alps:

Contributions to Mineralogy and Petrology, v. 135, p. 93–113, doi: 10.1007/s004100050500.

Jiang, W.-T., Peacor, D.R., Árkai, P., Tóth, M., and Kim, J.W., 1997, TEM and XRD determination of crystallite size and lattice strain as a function of illite crystallinity in pelitic rocks: Journal of Metamorphic Geology, v. 15, p. 267–281, doi: 10.1111/j.1525-1314.1997.00016.x.

Karlstrom, K.E., Heizler, M., and Quigley, M.C., 2010, Structure and ^{40}Ar/^{39}Ar K-feldspar thermal history of the Gold Butte block: Reevaluation of the tilted crustal section model, *in* Umhoefer, P.J., et al., eds., Miocene tectonics of the Lake Mead region, central Basin and Range: Geological Society of America Special Paper 463, p. 331–352, doi: 10.1130/2010.2463(15).

Lister, G.S., and Davis, G.A., 1989, The origin of metamorphic core complexes and detachment faults formed during Tertiary continental extension in the northern Colorado River region, U.S.A: Journal of Structural Geology, v. 11, p. 65–94, doi: 10.1016/0191-8141(89)90036-9.

McQuarrie, N., and Wernicke, B.P., 2005, An animated tectonic reconstruction of southwestern North America since 36 Ma: Geosphere, v. 1, p. 147–172, doi: 10.1130/GES00016.1.

Merriman, R.J., Roberts, B., and Peacor, D.R., 1990, A transmission electron microscope study of white mica crystallite size distribution in a mudstone to slate transitional sequence, North Wales, UK: Contributions to Mineralogy and Petrology, v. 106, p. 27–40, doi: 10.1007/BF00306406.

Michalski, J.R., Reynolds, S.J., Niles, P.B., Sharp, T.G., and Christensen, P.R., 2007, Alteration mineralogy in detachment zones: Insights from Swansea, Arizona: Geosphere, v. 3, p. 184–198, doi: 10.1130/GES00080.1.

Miller, E.L., Dumitru, T.A., Brown, R.W., and Gans, P.B., 1999, Rapid Miocene slip on the Snake Range–Deep Creek Range fault system, east-central Nevada: Geological Society of America Bulletin, v. 111, p. 886–905, doi: 10.1130/0016-7606(1999)111<0886:RMSOTS>2.3.CO;2.

Moore, D.M., and Reynolds, R.C., 1997, X-ray diffraction and the identification and analysis of clay minerals (second edition): New York, Oxford University Press, 378 p.

Mulch, A., Cosca, M.A., and Handy, M.R., 2002, In-situ UV-laser ^{40}Ar/^{39}Ar geochronology of a micaceous mylonite: An example of defect-enhanced argon loss: Contributions to Mineralogy and Petrology, v. 142, p. 738–752, doi: 10.1007/s00410-001-0325-6.

Myers, I.A., Smith, E.I., and Wyman, R.V., 1986, Control of gold mineralization at the Cyclopic Mine, Gold Basin district, Mohave County, Arizona: Economic Geology and the Bulletin of the Society of Economic Geologists, v. 81, p. 1553–1557, doi: 10.2113/gsecongeo.81.6.1553.

Numelin, T., Marone, C., and Kirby, E., 2007, Frictional properties of natural fault gouge from a low-angle normal fault, Panamint Valley, California: Tectonics, v. 26, TC2004, doi: 10.1029/2005TC001916.

Omar, G.I., Lutz, T.M., and Giegengack, R., 1994, Apatite fission-track evidence for Laramide and post-Laramide uplift and anomalous thermal regime at the Beartooth overthrust, Montana-Wyoming: Geological Society of America Bulletin, v. 106, p. 74–85, doi: 10.1130/0016-7606(1994)106<0074:AFTEFL>2.3.CO;2.

Pavlis, T.L., Serpa, L.F., and Keener, C., 1993, Role of seismogenic processes in fault-rock development: An example from Death Valley, California: Geology, v. 21, p. 267–270, doi: 10.1130/0091-7613(1993)021<0267:ROSPIF>2.3.CO;2.

Quigley, M.C., Karlstrom, K.E., Kelley, S., and Heizler, M., 2010, Timing and mechanisms of basement uplift and exhumation in the Colorado Plateau–Basin and Range transition zone, Virgin Mountain anticline, Nevada-Arizona, *in* Umhoefer, P.J., et al., eds., Miocene tectonics of the Lake Mead region, central Basin and Range: Geological Society of America Special Paper 463, p. 311–329, doi: 10.1130/2010.2463(14).

Reiners, P.W., Brady, R., Farley, K.A., Fryxell, J.E., Wernicke, B., and Lux, D., 2000, Helium and argon thermochronometry of the Gold Butte block, south Virgin Mountains, Nevada: Earth and Planetary Science Letters, v. 178, p. 315–326, doi: 10.1016/S0012-821X(00)00080-7.

Reiners, P.W., Farley, K.A., and Hickes, H.J., 2002, He diffusion and (U-Th)/He thermochronometry of zircon: Initial results from Fish Canyon Tuff and Gold Butte: Tectonophysics, v. 349, p. 297–308, doi: 10.1016/S0040-1951(02)00058-6.

Samson, S.D., and Alexander, E.C., 1987, Calibration of the interlaboratory ^{40}Ar-^{39}Ar dating standard, MMhb-1: Chemical Geology, v. 66, p. 27–34, doi: 10.1016/0168-9622(87)90025-X.

Solum, J.G., van der Pluijm, B.A., and Peacor, D.R., 2005, Neocrystallization, fabrics and age of clay minerals from an exposure of the Moab Fault, Utah: Journal of Structural Geology, v. 27, p. 1563–1576, doi: 10.1016/j.jsg.2005.05.002.

Spencer, J.E., and Welty, J.W., 1986, Possible controls of base- and precious-metal mineralization associated with Tertiary detachment faults in the lower Colorado River trough, Arizona and California: Geology, v. 14, p. 195–198, doi: 10.1130/0091-7613(1986)14<195:PCOBAP>2.0.CO;2.

Stockli, D.F., Surpless, B.E., Dumitru, T.A., and Farley, K.A., 2002, Thermochronological constraints on the timing and magnitude of Miocene and Pliocene extension in the central Wassuk Range, western Nevada: Tectonics, v. 21, 1028, doi: 10.1029/2001TC001295.

Tagami, T., 2005, Zircon fission-track thermochronology and applications to fault studies, *in* Reiners, P.W., and Ehlers, T.A., eds., Low-temperature thermochronology: Techniques, interpretations, and applications: Reviews in Mineralogy and Geochemistry Volume 58, p. 95–122, doi: 10.2138/rmg.2005.58.4.

Tagami, T., Lal, N., Sorkhabi, R.B., and Nishimura, S., 1988, Fission track thermochronologic analysis of the Ryoke Belt and the Median Tectonic Line, Southwest Japan: Journal of Geophysical Research, v. 93, no. B11, p. 13705–13713, doi: 10.1029/JB093iB11p13705.

Theodore, T.G., Blair, W.N., and Nash, J.T., 1987, Geology and gold mineralization of the Gold Basin–Lost Basin mining districts, Mohave County, Arizona: U.S. Geological Survey Professional Paper 1361, 167 p.

van der Pluijm, B.A., Hall, C.M., Vrolijk, P.J., Pevear, D.R., and Covey, M.C., 2001, The dating of shallow faults in the Earth's crust: Nature, v. 412, p. 172–175, doi: 10.1038/35084053.

Vrolijk, P., and van der Pluijm, B.A., 1999, Clay gouge: Journal of Structural Geology, v. 21, p. 1039–1048, doi: 10.1016/S0191-8141(99)00103-0.

Wasserburg, G.J., and Lanphere, M.A., 1965, Age determinations in the Precambrian of Arizona and Nevada: Geological Society of America Bulletin, v. 76, p. 735–758, doi: 10.1130/0016-7606(1965)76[735:ADITPO]2.0.CO;2.

Wernicke, B., and Axen, G.J., 1988, On the role of isostasy in the evolution of normal fault systems: Geology, v. 16, p. 848–851, doi: 10.1130/0091-7613(1988)016<0848:OTROII>2.3.CO;2.

Wernicke, B., Axen, G.J., and Snow, J.K., 1988, Basin and Range extensional tectonics at the latitude of Las Vegas: Geological Society of America Bulletin, v. 100, p. 1738–1757, doi: 10.1130/0016-7606(1988)100<1738:BARETA>2.3.CO;2.

Wright, L.A., and Troxel, B.W., 1993, Geologic map of the central and northern Funeral Mountains and adjacent areas, Death Valley region, southern California: U.S. Geological Survey Miscellaneous Investigations Series Map I-2305, scale 1:24,000.

Manuscript Received 25 May 2010
Revised Manuscript Received 24 February 2011
Manuscript Accepted 01 March 2011